Propagation Characteristics of Wideband Relay Channels in Urban Micro-Cell Environment

Jianhua Zhang, *Member, IEEE*, Di Dong, Yanping Liang, Chengxiang Huang, Guangyi Liu, *Member, IEEE*, and Weihui Dong

***Abstract*—In order to evaluate the performance of a relay system, propagation characteristics of relay channels are necessary, especially in urban micro-cell (UMi) environment. We conducted wideband relay channel measurements at 2.35 GHz in two UMi sites in China by employing a real-time channel sounder. Three types of links—base station to mobile station (BS–MS), relay station to mobile station (RS–MS), and base station to relay station (BS–RS)—were measured separately at three sites. Statistical propagation characteristics are presented and compared in this letter, including path loss (PL), root mean square (rms) delay spread (DS), and angular spread (AS). These results are informative for the technical research and evaluation of the relay system.**

***Index Terms*—Angular spread (AS), delay spread (DS), multiple-input–multiple-output (MIMO), path loss (PL), relay, wideband channel measurement.**

I. Introduction

RECENTLY, the relay system has attracted lots of attention as it has several advantages over conventional cellular system, such as coverage extension, capacity improvement, reduction in power consumption, and cooperative diversity gain [1], [2]. It is considered as one of the possible techniques for IMT-Advanced systems. However, the actual performance of a relay system highly depends on the channel conditions, such as large-scale fading and small-scale fading distribution. The large-scale fading effects are important for coverage prediction and interference analysis, and therefore crucial to the deployment of the relay system. Small-scale fading characteristics, including delay and angle of multipath components (MPCs), are necessary for the design of physical-layer transmission techniques. Thus, the propagation characteristics of relay channels should be exactly modeled in order to validate the system performance.

Manuscript received January 12, 2010; revised April 27, 2010; accepted June 14, 2010. Date of publication June 28, 2010; date of current version July 19, 2010. The research was supported in part by China Important National Science and Technology Specific Projects under No. 2009ZX03007-003-001 and by China 863 Program under No. 2009AA011502.

J. Zhang, D. Dong, and C. Huang are with Information and Telecommunications, Wireless Technique Innovation (WTI) Institute, Beijing University of Posts and Telecommunications, Beijing 100876, China (e-mail: jhzhang@bupt.edu.cn; dongdiunique@gmail.com; huangchengxiang86@126.com).

Y. Liang is with Information and Telecommunications, Wireless Technique Innovation (WTI) Institute, Beijing University of Posts and Telecommunications, Beijing 100876, China, and also with the Key Lab of Universal Wireless Communications, Ministry of Education, School of Information and Communication Engineering, Beijing 100081, China (e-mail: laodie0406@gmail.com).

G. Liu and W. Dong are with Research Institute of China Mobile, Beijing 100053, China (e-mail: liuguangyi@chinamobile.com; dongweihui@chinamobile.com).

Color versions of one or more of the figures in this letter are available online at http://ieeexplore.ieee.org.

Digital Object Identifier 10.1109/LAWP.2010.2054059

Most research about the relay system has been carried out under the simplified assumptions of relay channel properties [3]–[5]. The path loss (PL) of three separate links are supposed to follow the same propagation model, and the amplitude of each path is often assumed as Rayleigh-distributed. However, propagation characteristics of the relay channel are influenced by the geographic conditions and the antenna height of relay station (RS), base station (BS), and mobile station (MS). It raises a question whether the current model can be applied to the link from RS to MS since the antenna height at RS may be low under most circumstances [6]. Channel measurement is the most straightforward approach to obtain propagation characteristics. However, the difficulty to measure and model relay channel is that there exist two more links, i.e., RS–MS and BS–RS. A few relay channel measurements have been reported in [7] and [8], which mainly concentrated on the relay performance in indoor environments. An outdoor relay channel measurement is presented in [9], and it focused on fundamental deployment and multiantenna aspects. In this letter, statistical propagation characteristics based on the wideband relay channel measurements at 2.35 GHz in urban micro-cell (UMi) environment are presented and compared.

The rest of the letter is organized as follows. In Section II, the measurement system and environments are described. Section III presents the calculation approach of channel parameters. In Section IV, the channel characteristics are presented from three perspectives, i.e., PL, root mean square (rms) delay spread (DS), and angular spread (AS). Finally, conclusions are drawn in Section V.

II. Measurements Description

A. Measurement System

Channel impulse responses (CIR) were obtained utilizing the Elektrobit Propsound Channel Sounder. A pseudorandom sequence of length 1023 was continuously generated at the transmitter (TX) with a chip rate of 100 MHz. At the receiver (RX), CIRs were obtained by slide correlating the received signal with a synchronized copy of the sequence. The channel sampling frequency was 120.98 Hz. Different antenna configurations were applied for different measurement purpose: A single vertical-polarized dipole was employed at the BS, RS, and MS, respectively, in order to capture the large-scale and delay domain parameters; instead, to obtain the spatial domain parameters, omnidirectional array (ODA) consisting of 16 antenna elements aligned in a circle was utilized. The transmit power at the antenna input was 26 dBm.

(a)

(b)

Fig. 1. Measurement environment and route plans at three sites. (a) Site 1 and 2. (b) Site 3.

TABLE I
DETAILED MEASUREMENT INFORMATION

Items	S1	S2	S3
BS antenna height	20 m	20 m	22 m
RS antenna height	6.8 m	7.0 m	7.0 m
MS antenna height	1.8 m	1.8 m	1.8 m
BS-RS distance	144 m	58 m	106 m
BS-RS propagation condition	NLOS	LOS	LOS
Number of antennas (BS, RS, MS)	1,1,1	1,1,1	16,16,16

B. Measurement Environment

Measurements were performed at three measurement sites, which are denoted as S1, S2, and S3, respectively. Fig. 1(a) and (b) show the air views of the measurement environment. The detailed measurement information is listed in Table I. S1 and S2 were located on the campus of Beijing University of Posts and Telecommunications (BUPT), China. The average building height was 20 m. S3 was located in downtown Beijing, where buildings formed a Manhattan Grid with the average building height of 25 m. In S1, the BS (BS1) antenna was mounted on the rooftop of a building. The RS (RS1) antenna was located on the north side of the gymnasium. The BS (BS2) antenna in S2 was on the same rooftop just a few meters away from BS1, and the RS (RS2) antenna was installed on the west stand of the playground. As for S3, the BS (BS3) antenna is deployed on top of a five-floor-high building. The RS antenna was fixed on the top of a testing vehicle.

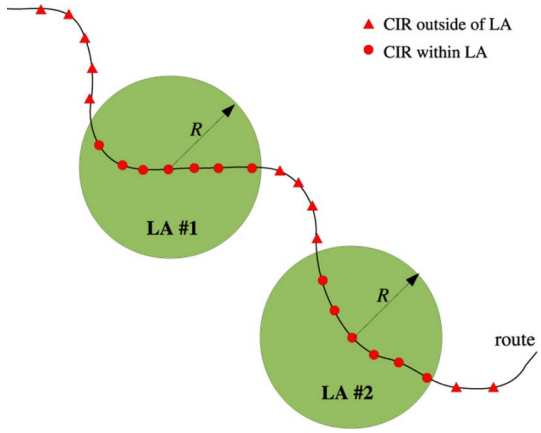

Fig. 2. Definition of LA along the measurement route.

As the average building height around S1, S2, and S3 is not below the BS antenna height, the propagation environment can be categorized into typical UMi. Considering that the height of the relay antenna does not need to be as high as the BS in order to reduce operating and maintenance costs [10], the antenna heights of RS1, RS2, and RS3 were set to 6.8, 7.0, and 7.0 m, respectively. The MS antenna was fixed on a trolley, moving at a velocity of about 0.5 m/s along the measurement routes. In Fig. 1(a), the solid line and dashed line represent measurement routes for S1 and S2, respectively. The corresponding number of sampling points per meter is about 242. MS positions were recorded using the GPS with the accuracy of several meters. As the relay is expected to cover a smaller region compared to the BS [1], the maximum distance between TX and RX in the measurement was about 250 m.

III. CALCULATION OF CHANNEL PARAMETERS

After the measurement, post-processing was implemented to obtain the channel parameters. In order to separate the noise from the measured MPCs, the dynamic range is set as 20 dB from the strongest path for both line-of-sight (LOS) and non-line-of-sight (NLOS) cases [11], [12]. In this section, the calculation procedures for PL, rms DS, and AS are presented.

A. Path Loss

PL is extracted from a set of small areas called *local area* (LA), where only small-scale fading takes place. Here, LA is defined as a disk with the radius of 10 λ, corresponding to 1.28 m at 2.35 GHz. Each channel snapshot location is the center of a corresponding LA, indicating that measurement routes will pass through a series of LAs. Fig. 2 illustrates the definition of LA.

Define the vector $\boldsymbol{r} = (x, y)$ as the location of MS at any instance with the coordinates of RS as (0,0). We use the expression in [13], letting $\mathcal{A}(\boldsymbol{r}; R) = \{\boldsymbol{s}_1, \boldsymbol{s}_2, \ldots, \boldsymbol{s}_N\}$ be the set of

measurement positions within the LA centered at $\boldsymbol{r}$ of radius R, where N is the cardinality of $\mathcal{A}(\boldsymbol{r};R)$. The joint effect of PL, shadow fading (SF), and antenna gain is written as

$$E(\boldsymbol{r}) = \frac{1}{N}\sum_{n=1}^{N}\int |h(\tau;\boldsymbol{s}_n)|^2 \mathrm{d}\tau, \quad \boldsymbol{s}_n \in \mathcal{A}(\boldsymbol{r};R) \tag{1}$$

where $h(\tau;\boldsymbol{s}_n)$ is the nth CIR within the local area. Denote the PL, SF, and antenna gain as $L(\boldsymbol{r})$, $S(\boldsymbol{r})$, and G_A, respectively, all in decibels. The PL in decibel without antenna gain is given by

$$L_{\mathrm{C}}(\boldsymbol{r}) = L(\boldsymbol{r}) + S(\boldsymbol{r}) = G_A - E_{\mathrm{dB}}(\boldsymbol{r}) \tag{2}$$

where $E_{\mathrm{dB}}(\boldsymbol{r})$ is $E(\boldsymbol{r})$ in decibels.

The single-slope log-distance model is adopted to estimate the PL for both LOS and NLOS cases. It is expressed as

$$L(\boldsymbol{r}) = a + 10n \cdot \log_{10} \|\boldsymbol{r}\| \tag{3}$$

where n and a are the PL exponent and intercept, respectively. $\|\boldsymbol{r}\|$ represents the TX–RX distance in meters. Then, linear regression in a minimum mean square error sense is implemented to estimate a and n. Finally, SF at position $\boldsymbol{r}$ can be obtained by subtracting the estimated PL component $L(\boldsymbol{r})$ from the power loss $L_{\mathrm{C}}(\boldsymbol{r})$.

B. Delay Spread

The rms DS is determined by the power delay profile at the LA. It is calculated as the standard deviation of the excess delay weighted with the power, which is given by

$$\tau_{\mathrm{rms}} = \sqrt{\left(\sum_{l=1}^{L} P_l\right)^{-1} \sum_{l=1}^{L} P_l \tau_l^2 - \left(\sum_{l=1}^{L} P_l\right)^{-2} \left(\sum_{l=1}^{L} P_l \tau_l\right)^2} \tag{4}$$

where τ_l and P_l denote, respectively, the excess delay and power of the lth path.

C. Angular Spread

AS evaluates the dispersion in angular domain and is calculated as the root second central moment of power angular spectrum. To avoid the ambiguous effect introduced by the circular wrapping of the angles, the circular AS (CAS) is calculated. This AS is constant regardless of the value of the angle shift, as in the case described in the 3 GPP spatial channel model (SCM) specifications [14]. The CAS is defined as

$$\sigma_{\mathrm{AS}} = \arg\min_{\Delta} \sigma_{\mathrm{AS}}(\Delta) = \sqrt{\sum_{l=1}^{L} \theta_{l,\mu}(\Delta)^2 P_l \cdot \left(\sum_{l=1}^{L} P_l\right)^{-1}} \tag{5}$$

where P_l is the power of the lth path. $\theta_{l,\mu}(\Delta)$ is given by

$$\theta_{l,\mu}(\Delta) = \begin{cases} 2\pi + \omega, & \omega < -\pi \\ \omega, & -\pi \leqslant \omega \leqslant \pi \\ 2\pi - \omega, & \omega > \pi \end{cases} \tag{6}$$

where ω can be written as

$$\omega = \theta_l(\Delta) - \sqrt{\sum_{l=1}^{L} \theta_l(\Delta) P_l \cdot \left(\sum_{l=1}^{L} P_l\right)^{-1}} \tag{7}$$

$$\theta_l(\Delta) = \theta_l + \Delta. \tag{8}$$

in which θ_l is the angle of the lth path estimated by Spatial-Alternating Generalized Expectation-maximization (SAGE) [15] algorithm and Δ denotes the angle shift ranging from $-\pi$ to π.

IV. Measurement Results and Discussion

A. Path Loss and Shadow Fading

The measured power loss of the RS–MS link and the estimated PL are shown in Fig. 3(a) and (b) for both LOS and NLOS cases, respectively. In the case of LOS, the results from S1 and S2 are plotted together. The estimated PL exponent is 2.09, which is quite close to that of the free-space model, and the intercept is 40.5. Since the antenna height of RS is below the average building height, UMi PL model recommended by ITU-R [16] and the IEEE 802.16j Type-F PL model [6] are selected for comparison. It is noticed that the UMi LOS model is below the free-space model and is also about 3 dB below the estimated PL. It indicates that the UMi LOS model may underestimate the PL within a short distance range when applied to the RS–MS link. Comparatively, the 802.16j model provides a better prediction.

As for the NLOS case, the number of power loss samples is fewer due to the power constraint at TX. The NLOS PL model for IEEE 802.16j Type-F scenario is geometry-based, which is difficult to be compared to our results when the MS was obstructed by irregular-shaped objects like trees and cars. Therefore, only the UMi PL model is chosen. Although the lower antenna height may lead to higher PL, our result shows that the estimated PL is below the UMi NLOS model when the TX–RX distance is less than 177 m. However, the estimated PL exponent is 4.64, which makes the PL exceed the UMi NLOS model when the distance reaches 177 m and farther. This is owing to the fact that the main obstructing objects located at a short distance in the measurement environment were trees and traffic, which caused less power attenuation, while the buildings were located at the edge of the coverage area. The intercept is 10.6. In general, the estimated PL and the UMi NLOS model are fairly close within the measurement range.

The SF in decibels can be well modeled as a zero mean Gaussian random variable. The standard deviation of the overall SF is 3.1 dB.

B. Delay Spread

Log-normal distribution is traditionally applied to describe the behavior of random rms DS. The empirical statistics of rms DS are listed in Table II, where various links involved in RS are compared. The μ_τ and σ_τ denote the fitting results of mean value and standard deviation, respectively. $\overline{\tau}$ is the mean value calculated from all samples of rms DS.

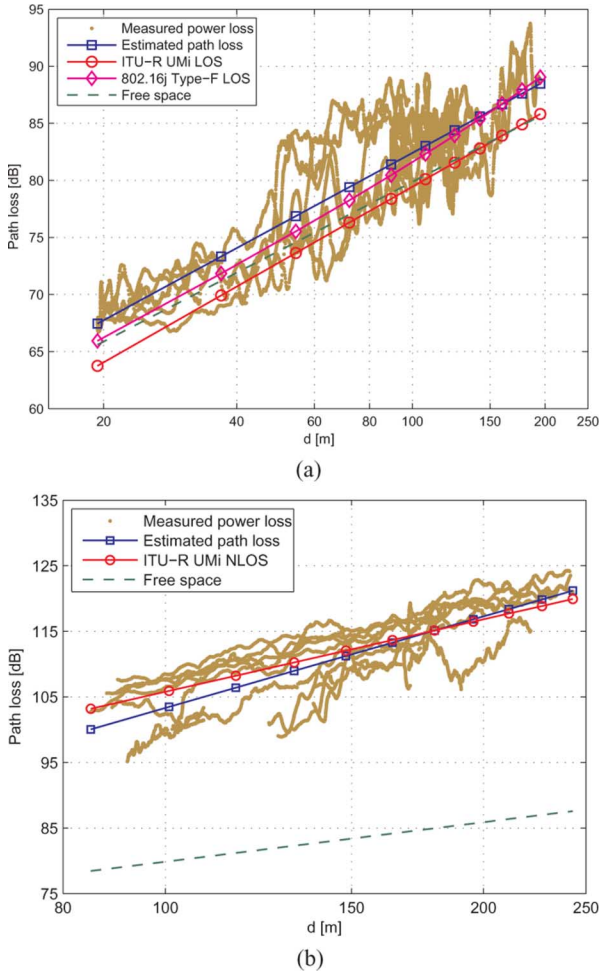

Fig. 3. PL of the RS–MS link for (a) LOS and (b) NLOS cases.

In the LOS case, the behaviors of rms DS for BS–MS and RS–MS links are similar since approximate statistical parameters are observed. Due to the existence of dominant component, the impacts of variation in dispersion paths are not evident, whereas in NLOS environment, the mean value of $\overline{\tau}$ decreases from 373 ns of the BS–MS link to 158 ns in the RS-MS case. The result indicates that introducing RS achieves considerable reduction of DS. The main reason involves the decrease of TX–RX distance.

In BS–RS link, however, the log-normal distribution can no longer fit the randomization of rms DS. Actually, the rms DS exists at 15 ns with a probability up to 68% in the fixed-fixed link. We thus propose to treat it as an invariable parameter in channel modeling.

C. Angular Spread

Table III depicts the statistics of the CAS of RS–MS link obtained from the measurement at S3. In the table, μ_A and σ_A are the parameters of the log-normal distributions when they are fitted to the CAS observations. The results demonstrate that at the same side, the CAS in the NLOS case is larger than that in the LOS case. It indicates that in the NLOS case, the dominant component does not exist. Instead, all MPCs are scattered

TABLE II
EMPIRICAL STATISTICS OF RMS DS FOR VARIOUS LINKS

Link		μ_τ [lg(s)]	σ_τ [lg(s)]	$\overline{\tau}$ [ns]
LOS	BS-MS	-7.03	0.26	96
	RS-MS	-7.05	0.26	95
NLOS	BS-MS	-6.44	0.08	373
	RS-MS	-6.83	0.18	158
BS-RS		–	–	15

TABLE III
STATISTICAL COMPARISON BETWEEN THE MEASURED CAS OF RS–MS LINK AND ITU STANDARD

link		RS-MS		ITU-R [16]	
propagation condition		LOS	NLOS	LOS	NLOS
CAS of AoD	μ_A [lg(deg)]	1.25	1.48	1.20	1.41
	σ_A [lg(deg)]	0.29	0.16	0.43	0.17
	mean[deg]	21.6	31.9	15.8	25.7
CAS of AoA	μ_A [lg(deg)]	1.40	1.56	1.75	1.84
	σ_A [lg(deg)]	0.24	0.18	0.19	0.15
	mean[deg]	28.5	38.9	56.2	69.2

throughout the propagation so that they are of similar power but distinct angle of arrival (AoA) and angle of departure (AoD). The results also represent that the CAS of AoA is larger than that of AoD for both LOS and NLOS scenarios. It is reasonable, as there are richer local scatterers along the mobile route for the MS than that surrounding the fixed RS. By contrast to the UMi scenario described in ITU-R [16], the CAS of AoD is larger in both LOS and NLOS cases. One reason resulting in this effect could be the fact that the antenna height of the RS is lower than that of BS in UMi environment. As a consequence, the MPCs interact with more scatterers within the local area when transmitted from the RS, which lead to larger CAS. On the contrary, the observed CAS of the AoA is smaller than that in the UMi scenario described in ITU-R [16]. It could be due to the fact that in the considered environment, the MS moves in the street canyon, thus the streets perform a wave-guided effect, which makes most of the MPCs impinge at the MS within a small range in the angular domain.

V. CONCLUSION

This letter presents characteristics of relay channels in two UMi sites in China. Based on the extensive channel measurements, parameters of the empirical log-distance PL models are obtained. Measurement results showed that the current IMT-Advanced channel model may underestimate the PL at a short TX–RX distance for the LOS case. The estimated PL exponent for the NLOS case was also larger than that in the current model. Moreover, in the LOS case, the behaviors of rms DS for BS–MS and RS–MS links are similar, and in NLOS case, the mean value of rms DS decreases from 373 ns of the BS–MS link to 158 ns in the RS-MS case. Compared to the current IMT-Advanced channel model, the CAS of AoD is larger in both LOS and NLOS cases. On the contrary, the observed CAS of AoA is smaller than that of IMT-Advanced channel model.

REFERENCES

[1] A. Nosratinia, T. E. Hunter, and A. Hedayat, "Cooperative communication in wireless networks," *IEEE Commun. Mag.*, vol. 42, no. 10, pp. 74–80, Oct. 2004.

[2] J. N. Laneman, D. N. C. Tse, and G. W. Wornell, "Cooperative diversity in wireless networks: Efficient protocols and outage behavior," *IEEE Trans. Inf. Theory*, vol. 50, no. 12, pp. 3062–3080, Dec. 2004.

[3] J. N. Laneman, G. W. Wornell, and D. N. C. Tse, "An efficient protocol for realizing cooperative diversity in wireless networks," in *Proc. IEEE ISIT*, 2001, pp. 294–294.

[4] R. Nabar, H. Bolcskei, and F. Kneubuhler, "Fading relay channels: Performance limits and space-time signal design," *IEEE J. Sel. Areas Commun.*, vol. 22, no. 6, pp. 1099–1109, Aug. 2004.

[5] B. Wang, J. Zhang, and A. Host-Madsen, "On the capacity of MIMO relay channels," *IEEE Trans. Inf. Theory*, vol. 51, no. 1, pp. 29–43, Jan. 2005.

[6] "Multi-hop relay system evaluation methodology (Channel model and performance metric)," IEEE 802.16j-06/013r3, 2007 [Online]. Available: http://wirelessman.org/relay/docs/80216j-06_013r3.pdf

[7] P. Kyritsi, P. Eggers, R. Gall, and J. Lourenco, "Measurement based investigation of cooperative relaying," in *Proc. IEEE VTC*, 2006, pp. 1–5.

[8] Y. Haneda, V. Kolmonen, and T. Riihonen, "Evaluation of relay transmission in outdoor-to-indoor propagation channels," [Online]. Available: http://www.cost2100.org/uploads/File/Workshop/Proceedings/W08114.pdf

[9] L. Jiang, L. Thiele, and V. Jungnickel, "Modeling and measurement of MIMO relay channels," in *Proc. IEEE VTC*, 2008, pp. 419–423.

[10] R. Pabst *et al.*, "Relay-based deployment concepts for wireless and mobile broadband radio," *IEEE Commun. Mag.*, vol. 42, no. 9, pp. 80–89, Sep. 2004.

[11] X. Zhao, J. Kivinen, P. Vainikainen, and K. Skog, "Propagation characteristics for wideband outdoor mobile communications at 5.3 GHz," *IEEE J. Sel. Areas Commun.*, vol. 20, no. 3, pp. 507–514, Apr. 2002.

[12] J. F. Kepler, T. P. Krauss, and S. Mukthavaram, "Delay spread measurements on a wideband mimo channel at 3.7 GHz," in *Proc. 56th IEEE VTC*, Sep. 2002, vol. 4, pp. 2498–2502.

[13] Y. Zhang *et al.*, "A novel spatial autocorrelation model of shadow fading in urban macro environments," in *Proc. IEEE GLOBECOM*, 2008, pp. 1–5.

[14] "Spatial channel model for multiple input multiple output (MIMO) simulations," 3rd Generation Partnership Project (3GPP), Tech. Rep. TR 25.996V8.0.0, 2009.

[15] B. H. Fleury *et al.*, "Channel parameter estimation in mobile radio environments using the sage algorithm," *IEEE J. Sel. Areas Commun.*, vol. 17, no. 3, pp. 434–450, Mar. 1999.

[16] "Guidelines for evaluation of radio interface technologies for IMT-Advanced," Rep. ITU-R M.2135, 2008.